http://ijeecs.iaescore.com | ISSN 2502-4752, e-ISSN 2502-4760

Indonesian Journal of Electrical Engineering and Computer Science

SJR SCImago Journal & Country Rank | Scopus

Q3 Computer Networks and Communications | SJR 2020 0.241 | SNIP 2020 0.635 | CiteScore 2020 2.0

Vol 22, No 1

April 2021

DOI: http://doi.org/10.11591/ijeecs.v22.i1

Table of Contents

Application of computational methods for harmonic state estimation of power system networks — PDF 1-9
Hassan Saadallah Naji, Husham Idan Hussein

Clusterization of customer energy usage to detect power shrinkage in an effort to increase the efficiency of electric energy consumption — PDF 10-17
Yessy Asri, Dwina Kuswardani, Efy Yosrita, Ferdinand Hendrik Wullur

IoT and transparent solar cell based automated green house monitoring system for tomato plant cultivation — PDF 18-27
Yus Rama Denny, Endi Permata, Adhitya Trenggono, Vaka Gustiono

Methodology to improve the accuracy of the model in photovoltaic systems — PDF 28-37
Jose Galarza

Developing collaboration tool for virtual team using UML models — PDF 38-44
Yasmin Makki Mohialden, Huda Abdulaali abdulbaqi, Narjis Mezaal Shati

Energy audit: types, scope, methodology and report structure — PDF 45-52
Pankaj Sharma, Surender Reddy Salkuti, Seong-Cheol Kim

Geometric control of quadrotor UAVs using integral backstepping — PDF 53-61
Ali Bouchaib, Rachid Taleb, Ahmed Massoum, Saad Mekhilef

Design and analysis of RNS-based sign detector for moduli set {2^n, 2^n - 1, 2^n + 1} — PDF 62-70
Raj Kumar, Ram Awadh Mishra

Real-time FPGA implementation of concatenated AES and IDEA cryptography system — PDF 71-82
Sara M. Hassan, Gihan. G. Hamza

Denoising of EEG signal based on word imagination using ICA for artifact and noise removal on unspoken speech — PDF 83-88
Efy Yosrita, Rosida Nur Aziza, Rahma Farah Ningrum, Givary Muhammad

Algorithmic TCAM on FPGA with data collision approach — PDF 89-96
Nguyen Trinh, Anh Le Thi Kim, Hung Nguyen, Linh Tran

Smart ambulance using IoT for blood transfer facilities — PDF 97-103
Mohamed A. Torad, Yahia H. Hossamel-din

Efficient TCAM design based on dual port SRAM on FPGA — PDF 104-112
Triet Nguyen, Kiet Ngo, Nguyen Trinh, Bao Bui, Linh Tran, Hoang Trang

Design, simulation and testing of an array of nano electro mechanical switches (NEMS) — PDF 113-120
Luay Mahdi, Qais Al-Gayem

Increasing transmission control protocol speed by reducing the acknowledgement collision probability — PDF 121-128
Suherman Suherman, Ali Hanafiah Rambe, Norshakila Haris, Anhar Anhar

Design and implementation of a stability control system for TCP/AQM network — PDF 129-136
Salam Waley Shneen, Mohammed Qasim Sulttan, Manal Kadhim Oudah

Simulation for determining the rod pump system parameter values using finite difference method
Erwani Merry Sartika, Arief Darmawan
PDF 137-145

Hybrid sliding PID controller for torsional vibrations mitigation in rotary drilling systems
Chafiaa Mendil, Madjid Kidouche, Mohamed Zinelabidine Doghmane
PDF 146-158

Delineation of electrocardiogram morphologies by using discrete wavelet transforms
Annisa Darmawahyuni, Siti Nurmaini, Hanif Habibie Supriansyah, Muhammad Irham Rizki Fauzi, Muhammad Naufal Rachmatullah, Firdaus Firdaus, Bambang Tutuko
PDF 159-167

Face Recognition with Frame size reduction and DCT compression using PCA algorithm
Padmaja vijaykumar, Jeevan K Mani
PDF 168-178

Classification of rice plant nitrogen nutrient status using k-nearest neighbors (k-NN) with light intensity data
Muliady Muliady, Lim Tien Sze, Koo Voon Chet, Suhadra Patra
PDF 179-186

Multimodal biometrics of fingerprint and signature recognition using multi-level feature fusion and deep learning techniques
Arjun Benagatte Channegowda, H N Prakash
PDF 187-195

Automated handwriting analysis based on pattern recognition: a survey
Samsuryadi Samsuryadi, Rudi Kurniawan, Fatma Susilawati Mohamad
PDF 196-206

Evaluation comparison of wave amount measurement results in brass-plated tire steel cord using RMSE and cosine similarity
April Lia Hananto, Sarina Sulaiman, Sigit Widiyanto, Aviv Yuniar Rahman
PDF 207-214

Enhancing the feature-based 3D deformable face recognition using hybrid PCA-NN
Cahyo Darujati, Supeno Mardi Susiki Nugroho, Deny Kurniawan, Mochamad Hariadi
PDF 215-221

Eye blink detection using CNN to detect drowsiness level in drivers for road safety
Pothuraju Vishesh, Raghavendra S, SantoshKumar Jankatti, Rekha V
PDF 222-231

SAR distribution of non-invasive hyperthermia with microstrip applicators on different breast cancer stages
Wong Vei Ling, Kasumawati Lias, Norlida Buniyamin, Hazrul Mohamed Basri, Mohammad Zulkaranen Ahmad Narihan
PDF 232-240

Efficient intelligent system for diagnosis pneumonia (SARS-COVID19) in X-Ray images empowered with initial clustering
Salam Saad Mohamed Ali, Ali Hakem Alsaeedi, Dhiah Al-Shammary, Hassan Hakem Alsaeedi, Hadeel Wajeeh Abid
PDF 241-251

Automated brain tumor classification using various deep learning models: a comparative study
Alaa Ahmed Abbood, Qahtan Makki Shallal, Mohammed Abdulraheem Fadhel
PDF 252-259

Classifying a type of brain disorder in children: an effective fMRI based deep attempt
Abeer M Mahmoud, Hanen Karamti
PDF 260-269

A composite controller based on nonlinear H ∞ and nonlinear disturbance observer for attitude stabilization of a flying robot
Vahid Razmavar, Heidar Ali Talebi, Farzaneh Abdollahi
PDF 270-276

Recently employed engineering techniques to reduce the spread of COVID-19 (corona virus disease 2019): a review study
Bander Saman, Mahmoud M. A. Eid, Marwa M. Eid
PDF 277-286

Basic FBG apodization functions effects on the filtered optical acoustic signal
Mahmoud M. A. Eid, Ahmed Nabih Zaki Rashed
PDF 287-296

A review of remote health monitoring based on internet of things
Omar AlShorman, Buthaynah Alshorman, Mahmoud Masadeh, Fahad Alkahtani, Basim Al-Absi
PDF 297-306

Generation and collection of data for normal and conflicting flows in software defined network flow table
Mutaz Hamed Hussien Khairi, Sharifah H. S. Ariffin, N. M. Abdul Latiff, Kamaludin Mohamad Yusof
PDF 307-314

Mobility-prediction and energy optimization for multi-channel multi-interface ad hoc networks in the presence of location errors
Hassan Faouzi, Mohammed Boutalline
PDF 315-325

Design and monitoring body temperature and heart rate in humans based on WSN using star topology
Setiyo Budiyanto, Freddy Artadima Silaban, Lukman Medriavin Silalahi, Selamet Kurniawan, Fajar Rahayu I. M., Ucuk Darusalam, Septi Andryana
PDF 326-334

Effect of controlling maximum-SNR-based relay selection strategy in cooperative wireless communication systems
Essam Saleh Altubaishi
PDF 335-341

Economic technology analysis of LTE advanced pro dual spectrum licensed and unlicensed access using discounted cash flow methods
Setiyo Budiyanto, Erman Al Hakim, Fajar Rahayu
PDF 342-351

Comparison of lithium niobate and silicon substrate on phase shift and efficiency performance for mach-zehnder interferometer modulator
Nor Hidayah Roslan, Aziati H. Awang, Mohd Hanapiah M. Yusoff, Ahmad Rifqi Md Zain
PDF 352-360

Adaptive security approach for wireless sensor network using RSA algorithm
Maha Salah Asaad, Muayad Sadik Croock
PDF 361-368

Dispersion compensation of optical systems utilizing fiber Bragg grating at 15 Gbits/s
Alaa Hussein Ali, Saad Mutashar, Ali Mahdi Hammadi
PDF 369-378

Mobility models for next generation wireless mesh network
Tsehay Admassu Assegie, Tamilarasi Suresh, R. Subhashni, Deepika M
PDF 379-384

Intelligent system for recruitment decision making using an alternative parallel-sequential genetic algorithm
Said Tkatek, Saadia Bahti, Otman Abdoun, Jaafar Abouchabaka
PDF 385-395

New efficient GAF routing protocol using an optimized weighted sum model in WSN
Hanane Aznaoui, Arif Ullah, Said Raghay, Layla Aziz, Mubashir Hayat Khan
PDF 396-406

Multi-constraints based RPL objective function with adaptive stability for high traffic IoT applications
Abdelhadi Eloudrhiri Hassani, Aicha Sahel, Abdelmajid Badri, El Mourabit Ilham
PDF 407-418

Unequal clustering in wireless sensor network: a review
Khalid Waleed Al-ani, Fairuz Bin Abdullah, Salman Yossuf
PDF 419-426

Particle swarm optimization for airlines fleet assignment
Abdallah A. Abouzeid, Mostafa Mohei Eldin, Mohammed Abdel Razek
PDF 427-434

Attitude on intention to use e-government in Indonesia
Dedy Afrizal, MUslimin Wallang
PDF 435-441

Embedding the three pass protocol messages into transmission control protocol header
Suherman Suherman, Deddy Dikmawanto, Syafruddin Hasan, Marwan Al-Akaidi
PDF 442-449

The trend malware source of IoT network
Susanto Susanto, M. Agus Syamsul Arifin, Deris Stiawan, Mohd. Yazid Idris, Rahmat Budiarto
PDF 450-459

Models of improved multilink reverse charging network by utilizing the bit error rate QoS attribute
Fitri Maya Puspita, Rohania Rohania, Evi Yuliza, Wenny Herlina, Yunita Yunita
PDF 460-468

Measuring information security policy compliance: content validity of questionnaire
Angraini Angraini, Rose Alinda Alias, Okfalisa Okfalisa
PDF 469-475

Analysis of sales levels of pharmaceutical products by using data mining algorithm C45
Rini Sovia, Abulwafa Muhammad, Syafri Arlis, Guslendra Guslendra, Sarjon Defit
PDF 476-484

Designing consensus algorithm for collaborative signature-based intrusion detection system
Eko Arip Winanto, Mohd Yazid Idris, Deris Stiawan, Mohammad Sulkhan Nurfatih
PDF 485-496

Service landscape for private universities in indonesia based on service oriented architecture and cloud technology
Faiza Renaldi, Irma Santikarama, Esmeralda C. Djamal, Agya Java Maulidin
PDF 497-506

Securing sensor data transmission with ethernet elliptic curve cryptography secure socket layer on STM32F103 device
Seniman Seniman, Baihaqi Siregar, Rani Masyithah Pelle, Fahmi Fahmi
PDF 507-515

Web-based document certification system with advanced encryption standard digital signature
Henny Indriyawati, Titin Winarti, Vensy Vydia
PDF 516-521

Pushing towards ehealth for iraqi hypertensives: an integrated class association rules into SECI model
Ahmed Aljuboori, Lubab Ahmed Tawfeeq, Khamis A. Al-Karawi
PDF 522-533

Air temperature prediction using different machine learning models
Rana Muhammad Adnan, Zhongmin Liang, Alban Kuriqi, Ozgur Kisi, Anurag Malik, Binquan Li, Fatemehsadat Mortazavizadeh
PDF 534-541

Organizing sports matches with a hybrid monkey search algorithm
Ruqaya Zedan Shaban, Isra Natheer Alkallak
PDF
542-551

A state-of-the-art survey on semantic similarity for document clustering using GloVe and density-based algorithms
Shapol M. Mohammed, Karwan Jacksi, Subhi R. M. Zeebaree
PDF
552-562

e-SimNet: a visual similar product recommender system for E-commerce
Ssvr Kumar Addagarla, Anthoniraj Amalanathan
PDF
563-570

Analysis of the performance of grounding grids buried in heterogeneous soil under impulse current
Amina Djaborebbi, Boubakeur Zegnini, Djillali Mahi
PDF
571-579

A survey on predicting oil spills by studying its causes using deep learning techniques
Mona Mohamed Nasr, Fahd Kamal Al-Sheref, Yasmen Samhan Abd Elwahab
580-589

Dispatching the problems in implementing mobile payment services from consumer attitude perspective
Hoang Thien Van, Vo Anh Tien, Huynh Cong Danh, Hoang-Sy Nguyen
PDF
590-597

Improved Lagrangian relaxation generation decision-support in presence of electric vehicles
Hossein Zeynal, Zuhaina Zakaria, Ahmad Kor
PDF
598-608

This work is licensed under a Creative Commons Attribution-ShareAlike 4.0 International License.

IJEECS visitor statistics

Indonesian Journal of Electrical Engineering and Computer Science
Vol. 22, No. 1, April 2021, pp. 137~145
ISSN: 2502-4752, DOI: 10.11591/ijeecs.v22.i1.pp137-145

Simulation for determining the rod pump system parameter values using finite difference method

Erwani Merry Sartika, Arief Darmawan
Department of Electrical Engineering, Universitas Kristen Maranatha, Indonesia

Article Info

Article history:

Received Feb 20, 2020
Revised Nov 10, 2020
Accepted Dec 5, 2020

Keywords:

Artificial lift
Lifting petroleum
Pump card
Rod pump
Simulation

ABSTRACT

Lifting petroleum to the surface requires a mechanism called an artificial lift. This mechanism is useful for increasing the flow of fluids from a well. One that uses this method is the rod pump. The rod pump system needed the appropriate design (through the determination of the value of the parameters that affect) so that the pump runs optimally. But changing the appropriate design in real terms is not economically and time-efficient. The ideal rod pump system analysis procedure is to take downhole data (in the well) which is commonly called a pump card. A pump card calculation simulation is needed to efficiently analyze the rod pump system. The wave equation can describe the model of the rod pump system. A simulation of pump data calculation is performed using the finite difference method for the wave equation solution. Through the process of tuning parameter values using trial and error methods, the steps of tuning the parameter value of the rod pump system are proposed in this paper. For further research, a pump card calculation method based on a surface card can be developed to efficiently analyze the rod pump.

This is an open access article under the CC BY-SA license.

Corresponding Author:

Erwani Merry Sartika
Department of Electrical Engineering
Universitas Kristen Maranatha
Jln. Suria Sumantri 65 Bandung, Indonesia
Email: erwanimerry@gmail.com

1. INTRODUCTION

At present, oil and gas are one of the energies that are still relied on by humans, so the demand for oil and gas is higher. However, to use it a special method is needed to transport this energy source. Therefore, to lift petroleum to the surface a mechanism called an artificial lift is needed. This mechanism is useful for increasing the flow of fluids from a well [1].

The pump is one of the industrial equipment that is widely used today, including in the oil and gas industry. Pump sucker or sucker rod pump is one type of pump in the upstream oil and gas industry that uses the method of artificial lift (power assistance) in the removal of petroleum from the well. This type of pump is usually used in wells that have particles in them and are often also applied to old wells [1]. Surface card data collection methods have been used to analyze the rod pump system. Interpretation of the actual pump conditions of the surface card is very difficult because the data are qualitative and depend on the expertise of the analyzer [2].

Therefore, an analysis procedure is used by taking downhole data (in the well) which is commonly called a pump card. A pump card calculation method based on a surface card is needed to efficiently analyze the actual pump rod system. A pump card calculation method based on a surface card is needed to be able to analyze the actual rod pump system efficiently [3]. Pump card data calculations using the finite difference method have been used to get solutions based on the wave equation [4].

Alternative system designs using simulations are carried out to get optimal results [5-8]. Through the pump card data, it is necessary to adjust the parameter values on the rod pump to obtain the ideal pump (optimal) [9]. But changing the parameter values that affect the rod pump in real terms is not economically and time-efficient [10]. Tuning parameter values is mostly done through direct data retrieval by conducting sonological tests to determine the bottom well flow pressure and reservoir pressure. Sonologists work on the principle of waves or sound from the firing or flowing of pressuized gas quickly. Redesign the sucker rod pump without changing the type of pump installed by combining the step length and pump speed, so that volumetric pumping and pump displacement efficiency are obtained based on direct data collection [11].

So, the purpose of this paper is to use simulations to determine the parameter values on the rod pump to get the ideal pump card. Through this simulation, in addition to saving costs and time, it can also be used to anticipate the rod pump if the pump card is not ideal (because it can damage the rod pump). Parameters that can be adjusted and affect the output of the rod pump system is the length of the rod string, the diameter of the rod string, and the speed of the pump [11]. Determination of the parameter value on the rod pump in advance using the trial-and-error method. Through the trial and error method, an analysis is performed to obtain the stages of determining the tuning parameters to accelerate the acquisition of parameter values (through a simulation process).

2. WORKING PRINCIPLE OF ROD PUMP

The working mechanism of the rod pump is the working process of all the components contained in the pump shown in Figure 1 [12-14]. The workings of the pump shaft are divided into two, namely on the surface and in the well. The way the rod pump works on the surface is:

a) Prime motion (prime mover) will produce rotational motion, then this motion will be converted into up and down the motion by the pitman crank assembly system. Furthermore, this motion will go through a walking beam and forwarded to the horse head and made straight up and down to move the plunger inside the well.

b) Pumping unit installation above the surface is connected to the pump installation in the well by the sucker rod system, so that the straight up and down motion of the horse head will be moved to the pump plunger, and the plunger will move up and down in the pump barrel.

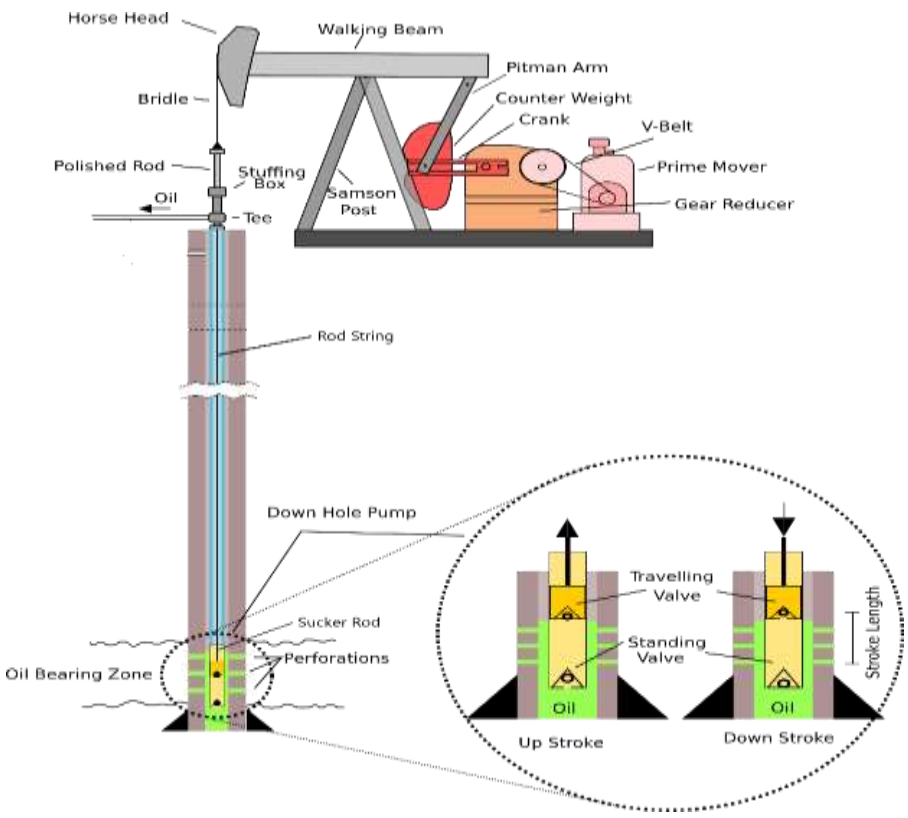

Figure 1. Rod pump components [9]

The way the rod pump works in the well is:

a) During an upstroke, the plunger will move upwards the traveling valve away from the standing valve, causing the traveling valve to be closed due to pressure from the fluid above it. The fluid can be lifted and out through the pipe. When the plunger moves upward, the pressure in the barrel will decrease to the vacuum pressure, so that the formation pressure will open the standing valve and the fluid will enter the barrel.

b) During the downstroke process, the standing valve will be closed due to the pressure of the liquid above it and the influence of the weight of the balls themselves, while the traveling valve will open and be pushed by the liquid inside the barrel, then the liquid will enter the tubing and lifted due to the pump surface movement. This process will continue until the pipe is filled with fluid and moves to the surface.

3. DYNAMOMETER CARD

Dynamometer card is divided into 2 namely surface card and pump card. The surface card displays the load on the rod during the pump cycle and is converted to a pump card that displays the fluid load on the pump during the pump cycle [15-16]. The size and shape of the card show the operating conditions and pump performance as shown in Figure 2. There are 4 points, or 4 sequences that occur when lifting oil. Point 1 to 3 is during the upstroke movement and point 3 to point 1 is during the downstroke movement. Fo (fluid load on the pump) is the process of transferring the valve to fill fluid into the working barrel. Stroke length effective plunger travel (SLEPT), which is the effective stroke length to form the ideal pump card, only occurs when one valve is open and the other closed. Stroke length downhole (SLDH), which is the total stroke length of the downhole plunger [17].

The surface card is the recording of the load on the polished rod against the displacement of the position of the sucker rod which is commonly called the rod through physical sensors mounted on the polished rod. The wave equation is a mathematical model that can estimate the motion of the rod against conditions in the well [18]. A pump card is the recording of the load at the downhole against the displacement of the rod [19].

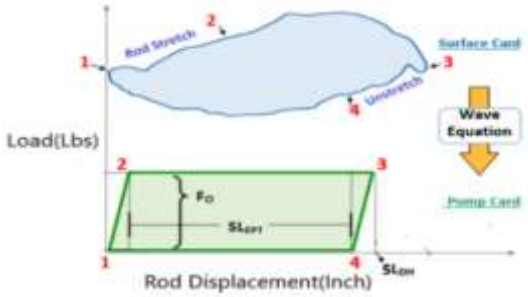

Figure 2. Surface card and pump card [17]

4. PUMP CARD

Interpretation of the actual pump conditions of surface cards is very difficult because the data are qualitative and depend on the expertise of the analyzer. The ideal analysis procedure is to take downhole data (under the well) which is commonly called a pump card. There are types of pump cards according to rod pump work and well conditions [17]:

Ideal card: normal pump, full liquid & no gas interference. The pump is functioning properly

Slanted: there is gas interference which causes a shift in the tubing when lifting

Fluid pound: during downsroke there is an empty space so that it can cause the rod to break when it collides with fluid

5. THE WAVE EQUATIONS

The wave equation is ideal for representing rod movement because it involves wave propagation in continuous media. The wave equation for the rod pump is expressed by (1) [20].

$$v^2 \frac{\partial u(x,t)}{\partial x^2} = \frac{\partial^2 u(x,t)}{\partial t^2} + c \frac{\partial (x,t)}{\partial t} \quad (1)$$

In (1) is the wave equation which states that the motion of the rod is not affected by the diameter of the rod string. The wave equation that states the motion of the rod can be affected by the diameter of the rod string can be expressed in (2) [20].

$$EA \frac{\partial^2 u(x,t)}{\partial x^2} = \frac{\rho A}{144 g_c} \frac{\partial^2 u(x,t)}{\partial t^2} + c \frac{\rho A}{144 g_c} \frac{\partial u(x,t)}{\partial t} \quad (2)$$

E = Modulus Young (Psi)
A = Transversal Area (inch2)
ρ = Thickness (lb / ft3)
g_c= Conversion Factor (lbm * ft / lbf / s2) = 32.2
c = damping coefficient (s-1)
v = Velocity (ft / sec)
u = Rod Displacement

The finite difference method is a method for obtaining numerical solutions of partial differential equations [21]. Estimated results of wave equations are discretized using finite difference as shown in (3) [20].

$$u_{i+1,j} = \left[\frac{\alpha\,(1+c\Delta t)}{\beta}\right] u_{i,j+1} - \left[\frac{\alpha\,(2+c\Delta t)-2\beta}{\beta}\right] u_{i,j} + \frac{\alpha}{\beta} u_{i,j-1} - u_{i-1,j} \quad (3)$$

$\alpha = \dfrac{\left(\frac{\Delta x}{\Delta t}\right)\rho A}{144 gc}$
$u_{0j} = g_{PR_j}$
$\beta = \dfrac{EA}{\Delta x}$
$U_{Ij} = \dfrac{f_{PR_j.\Delta_x}}{EA} + U_{O,J}$
g_{PR} = rod displacement in surface card
f_{PR} = fluid load in surface card

The final calculation for rod displacement and fluid load uses (4) and (5) [20] :

$$u_{pump,j} = (1 + c\Delta t)u_{m-1,j+1} - c\Delta t u_{m-1,j} + u_{m-1,j-1} - u_{m-2,j} \quad (4)$$

$$F_{pump,j} = \left(\frac{EA}{2\Delta x}\right)\left(3u_{m,j} - 4u_{m-1,j} + u_{m-2,j}\right) \quad (5)$$

U = rod displacement on pump card
F = fluid load on pump card

6. RESEARCH METHOD

In designing the pump card calculation simulation is divided into three main stages. The first step is to convert the surface card data into pump card data using the wave equation. After getting the pump card data, the parameter data that affects the rod pump system is adjusted. The last step is to analyze the results of the simulation of the rod pump system based on the pump card data.

The surface card image is taken from the database based on references as shown in Figure 3 [22]. Surface card data is in the form of data pairs X and Y, each of which has 500 points. X is the displacement data rod and Y is the data load. It is assumed that the simulation of one cycle of the rod pump system is 360 points (one full rotation of the 360° motor). Followed by making a matrix of M rows of 100, and N columns of 360 and input NaN (not a number) data to allocate initial condition data from the matrix. Initialization of

the first row and the second row of the matrix. The wave equation is used to get the next row (third row to the last row) as shown in the flow diagram of rod pump system simulation in Figure 4.

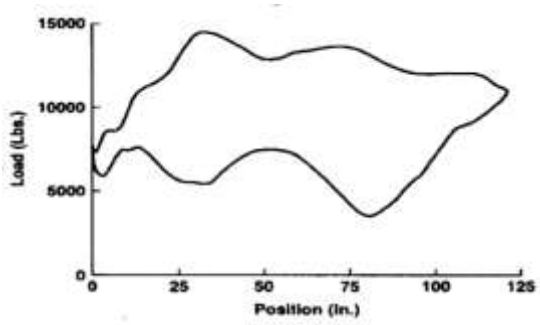

Figure 3. Surface card image[22]

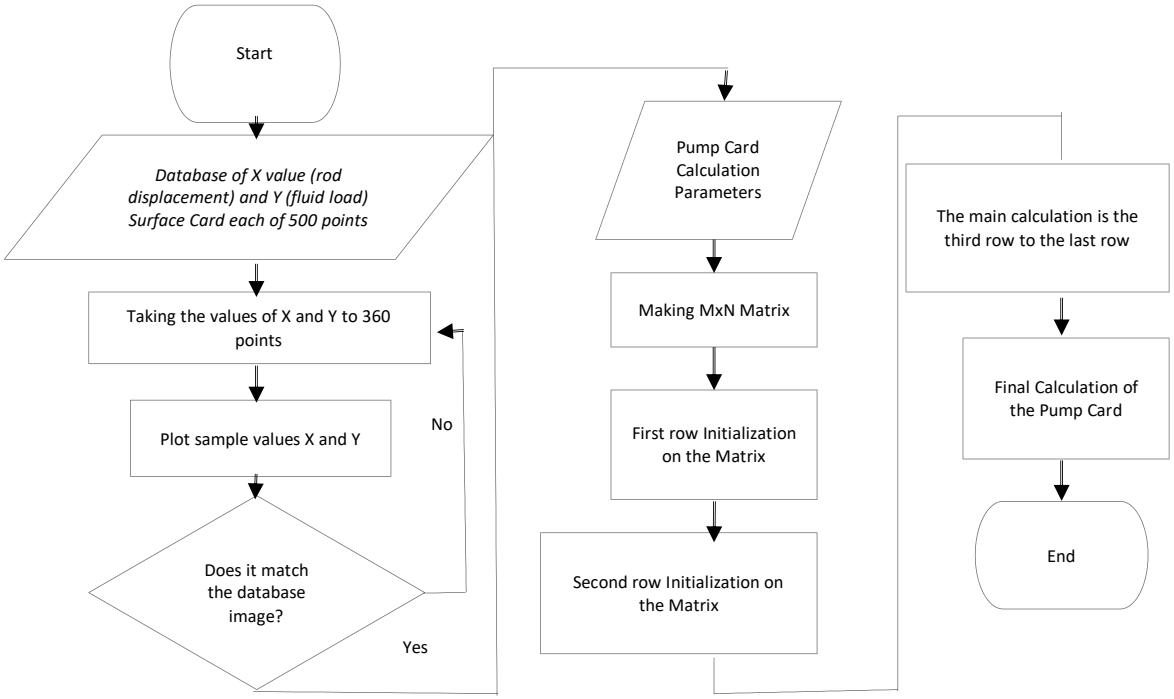

Figure 4. Flow diagram of rod pump system simulation

The parameters used for pump card data calculations can be seen in Table 1. The parameters that will be used as reference parameters for the rod pump system are the parameters of rod string length, rod string diameter, and pump speed because these parameters are parameters that can be changed for the system design rod pump. The other parameters are fixed parameters that cannot be changed [23].

Figure 5 is the final result of the pump card calculation process using a wave equation that has been discretized. The column in the matrix is increased to 720 because if the calculation starts from the surface node (i = 0) with only one cycle until the pump solution (i = m) will not represent a complete cycle because to get the main calculation current data and previous data are needed. 360 data columns of the first cycle will be used as current data and previous data to be able to calculate the data that will come incomplete so that no data is lost.

The first row in the matrix is the initialization of the data displacement rod on the surface card. The second row is initializing fluid load data plus data rod displacement on the surface card. The third row to the m-row is the main calculation using the wave equation that has been discretized using finite-difference. NaN is the IEEE arithmetic representation for Not-a-Number [24]. NaN is used to allocating initial condition data from the matrix (because it cannot be a number including zero) [25].

Table 1. The parameters used for pump card calculation simulation [23]

Parameter	Description
E	Modulus Young (Psi) = $30{,}5.10^6$
A	Transversal Area ($inch^2$) = π / (4. (diameter)^2)
L	Rod String Length (ft) = Parameters to be set
v	Speed in one cycle (SPM) = Parameters to be set
D	Diameter of rod string (inch) = Parameters to be set
m	Number of matrix rows for pump card data calculation = 100
n	Number of matrix columns for calculation of pump card data = 360
c	The damping coefficient (s^{-1}) = 0,8
ρ	Viscosity (lb / ft3) = 490
g_c	Conversion Factor (lbm.ft/lbf/s^2) = 32.2

180x720																	
	1	2	3	...	177	178	179	180	...	541	542	543	544	...	718	719	720
1	0.0456	0.0465	0.0491	...	0.1156	0.1320	0.1501	0.1699	...	0.1914	0.1699	0.1501	0.1320	...	0.0534	0.0491	0.0465
2	0.0583	0.0592	0.0618	...	0.1284	0.1448	0.1631	0.1831	...	0.2007	0.1793	0.1596	0.1416	...	0.0652	0.0614	0.0591
3	NaN	0.0720	0.0745	...	0.1411	0.1576	0.1760	0.1963	...	0.2100	0.1887	0.1691	0.1513	...	0.0771	0.0737	NaN
4	NaN	NaN	0.0873	...	0.1539	0.1704	0.1890	0.2094	...	0.2194	0.1981	0.1786	0.1609	...	0.0889	NaN	NaN
5	NaN	NaN	NaN	...	0.1666	0.1832	0.2020	0.2226	...	0.2287	0.2076	0.1882	0.1705	...	NaN	NaN	NaN
6	NaN	NaN	NaN	...	0.1794	0.1961	0.2149	0.2358	...	0.2380	0.2170	0.1977	0.1802	...	NaN	NaN	NaN
7	NaN	NaN	NaN	...	0.1922	0.2089	0.2279	0.2490	...	0.2474	0.2264	0.2072	0.1898	...	NaN	NaN	NaN
8	NaN	NaN	NaN	...	0.2050	0.2218	0.2409	0.2622	...	0.2567	0.2358	0.2168	0.1994	...	NaN	NaN	NaN
⋮	⋮	⋮	⋮	⋮	⋮	⋮	⋮	⋮	⋮	⋮	⋮	⋮	⋮		⋮	⋮	⋮
178	NaN	NaN	NaN	...	14.9752	14.9682	14.9594	14.9484	...	14.9358	14.9207	14.9033	14.8840	...	NaN	NaN	NaN
179	NaN	NaN	NaN	...	NaN	14.9876	14.9787	14.9677	...	14.9549	14.9398	14.9223	NaN	...	NaN	NaN	NaN
180	NaN	NaN	NaN	...	NaN	NaN	14.9980	14.9870	...	14.9741	14.9588	NaN	NaN	...	NaN	NaN	NaN

Figure 5. Matrix for pump card calculations

7. RESULTS AND ANALYSIS

The parameters that influence the formation of the pump card are rod string diameter, rod string length, transverse area, density, damping factor, conversion factor, modulus young, and pump speed. In the simulation that will be tuned are the parameters of the rod string diameter, the length of the rod string, and the speed of the pump as a mechanical design and the process of the rod pump system because the other parameters are fixed coefficients. The pump card data that shows the rod pump system works well is having a large net stroke, a small stroke shift, and a large fluid load with a note that the pump card shape must resemble a rectangle (ideal pump card). Net stroke is an effective stroke to transport the fluid, if the net stroke value increases, the fluid transported will be even greater. Gross stroke is the displacement of a stroke in one pump cycle. The total stroke shift is a gross stroke reduced by a net stroke which represents a stroke that deviates from normal conditions.

In the simulation of the rod pump system, it was conducted preliminary by trial and error method by adjusting the values of the various parameters of the rod pump namely the diameter of the rod string (0.625 inches; 0.750 inches; 0.875 inches), the length of the rod string (1000 ft; 2000 ft; 3000 ft), and the speed of the rod pump in one cycle (8 SPM to 20 SPM). From all trials in Table 2, the results of simulation data are shown which are considered to be representative of all experiments.

From Table 2 the analysis of the tuning process can be concluded. In the initial tuning of the rod string diameter and the length of the rod string, one can be chosen first, because this gives the same results as the effect on the net stroke size, stroke shift, and fluid load. Small diameter rod string and long rod string will produce a large net stroke, small stroke shift, and a large enough fluid load. Meanwhile, to find out the shape of a pump card resembling a rectangle (ideal pump card) is determined by the next step which is the value of the speed of the rod pump in one cycle (SPM).

Table 2. Simulation results of pump cards with rod string diameter 0.625 inches for various rod string lengths, rod string length 3,000 feet for various rod string diameters, and pump speed 8-20 spm

Rod String Diameter (Inch)	Length of the rod string (ft)	Speed (SPM)	*Net stroke* (inch)	*Gross Stroke* (inch)	Total Stroke Shift (Inch)	*Fluid load* (lbs)	Length of the rod string (ft)	Rod String Diameter (Inch)	Speed (SPM)	*Net stroke* (inch)	*Gross Stroke* (inch)	Total Stroke Shift (Inch)	*Fluid load* (lbs)
		8	71,2	133,3	62,1	11730			8	103,4	122,4	19	11850
		9	70,8	133,1	62,3	11930			9	104.5	120,3	15.8	12000
		10	70,5	133	62,5	11970			10	113	120,3	7.3	12200
		11	70,2	132,9	62,7	11980			11	114.4	120,8	6.4	12250
		12	69,8	132,7	62,9	12090			12	88,2	119,4	31,2	12400
		13	69,3	132,3	63	12130			13	87	118,8	31,8	12600
	1000	14	69	131,9	62,9	12160		0.625	14	82,5	118,2	35,7	12700
		15	68,8	131,6	62,8	12200			15	83,3	117,5	34,2	12700
		16	68,7	131,5	62,8	13220			16	82,1	116,9	34,8	12800
		17	68,5	131,1	62,6	13300			17	81,5	116	34,5	13000
		18	68,3	131,2	62,9	12350			18	80,9	116,2	35,3	13200
		19	68,2	130,9	62,7	12410			19	80,6	115,8	35,2	13500
		20	67,5	130,6	63,1	12450			20	80,2	115,8	35,6	13750
		8	89.8	126	36.2	11800			8	93,8	125,8	32	12200
		9	92.8	126	30.2	12000			9	94,5	125,3	30,8	12250
		10	93.3	125.5	30	12100			10	96,2	124,6	28,4	12350
		11	94.7	125.3	29.6	12500			11	91,9	124,1	32,2	12500
		12	95	125	29	12630			12	91,5	123,5	32	12750
		13	96.3	124.7	28.4	12700			13	90,6	123	32,4	12950
0.625	2000	14	96.5	124.3	27.8	12890	3000	0.750	14	87,7	122,3	34,6	13000
		15	96.8	123.8	27	13050			15	75,4	121,5	46,1	13200
		16	83.9	123.5	39.6	13300			16	74,9	120,7	45,8	13450
		17	82.7	123	40.3	14000			17	73,5	120,3	46,8	13750
		18	81.8	122.4	40.6	14100			18	72,1	120	47,9	14100
		19	80.9	121.8	40.9	14350			19	70,3	120,1	49,8	14300
		20	80.4	121.3	40.9	14600			20	67,3	118	50,7	14850
		8	103,4	122,4	19	11850			8	79	128,8	49,8	12400
		9	104.5	120,3	15.8	12000			9	83,6	128,2	44,6	12600
		10	113	120,3	7.3	12200			10	87,4	127,6	40,2	12750
		11	114.4	120,8	6.4	12250			11	69,5	126,7	57,2	12900
		12	88,2	119,4	31,2	12400			12	72	126,3	54,3	13200
		13	87	118,8	31,8	12600			13	71	125,5	54,5	13400
	3000	14	82,5	118,2	35,7	12700		0.875	14	70,1	124,8	54,7	13700
		15	83,3	117,5	34,2	12700			15	71	124,1	53,1	14100
		16	82,1	116,9	34,8	12800			16	71,3	123,2	51,9	14300
		17	81,5	116	34,5	13000			17	68,3	122,3	54	14800
		18	80,9	116,2	35,3	13200			18	66,2	121,7	55,5	15100
		19	80,6	115,8	35,2	13500			19	60	120,7	60,7	15400
		20	80,2	115,8	35,6	13750			20	58,5	119,8	61,3	15700

(a) (b)

Figure 6. (a) Pump card with a diameter of 0.625-inch rod string parameter, 2000 ft rod length, and 15 SPM speed. (b) Pump card with 0.625-inch diameter rod string parameters, 3000 ft rod length, and 11 SPM speed

Some forms of pump cards that are produced from simulations are shown in Figure 6(a) and Figure 6(b). The pump card closest to the ideal shape of the data in Table 3. is at the 15 SPM speed shown in Figure 6(a). At 0.625-inch rod string diameter, 2000 ft rod length, net stroke value was 96.8 inches, and the total stroke shift was 27 inches. In Figure 6(a) it is shown that the shape of the pump card has formed a rectangle but still needs to look for other values that have a squarer box shape (ideal pump card). The most approaching pump card the ideal shape of the data in Table 2, is at the speed of 11 SPM shown in Figure 6(b). At 0.625-inch rod string diameter, 3000 ft rod length, net stroke value is 114.4 inches, and the total stroke shift is 6.4 inches.

So the conclusion of the tuning process parameter values on the rod pump is:

1) Can choose the smallest rod string diameter or the longest rod string length for the initial selection of parameter values because both are linear to the net stroke:
   a) The smaller the diameter of the rod string, the bigger the net stroke
   b) The longer the rod string, the bigger the net stroke
2) If at the beginning choose the smallest rod string diameter, then select the longest rod string or if at the beginning choose the longest rod string, then select the smallest rod string diameter.
3) Then the speed selection (SPM) can then be adjusted from the smallest to the largest, but all conditions must be considered: first, having the largest net stroke, second having the smallest stroke shift, and the third one is having a large enough fluid load and became a square pump card (ideal pump card).

8. CONCLUSION

In this paper, a simulation was carried out to obtain the ideal pump card. Through the analysis of simulation results using the trial-and-error method, the tuning process of the parameter values used is to first choose the diameter of the rod string (selected small) and the length of the rod string (selected the longest), followed by the selection of the speed of the rod pump (SPM) which produces a sequence of the largest net stroke, shifting the smallest stroke, and fluid load large enough to approach the ideal shape of the pump card (rectangle). In other paper tuning parameters is done by taking data directly by performing a sonologist test to determine the bottom well flow pressure and reservoir pressure. Based on the simulation the diameter of the rod string is 0.625 inches, the length of the rod string is 3000 feet, and the pump speed of 11 SPM forms the ideal pump card. Based on the tuning process on the proposed rod pump, tuning is done by selecting the smallest rod string diameter and the longest length of the rod string, then continuing to determine the motor speed so that the most ideal pump card is obtained. For further research, a pump card calculation method based on the surface will be developed to analyze the efficiency of the rod pump. Simulation is used to adjust the rod pump parameters directly based on the surface card. In addition, further developments can take advantage of IoT for monitoring real conditions in the field (well conditions) to determine changes in parameter values that affect the performance of the rod pump system.

ACKNOWLEDGEMENTS

Thank you to PT Danfoss Indonesia for the opportunity given in researching this topic.

REFERENCES

[1] O. R. ; P. Almeida, "Numerical simulation of the sucker-rod pumping system Simulación numérica de un sistema de bombeo mecánico," *Ing. E Investig.*, vol. 34, pp. 4-11, 2014, doi: 10.15446/ing.investig.v34n3.40835.

[2] X. Xu, R. Gong, Y. Li, J. Li, Q. Li, and Z. Xu, "Binary Histogram of Oriented Gradients Based Dynamometer Card Recognition," in *Proceedings - 13th International Conference on Computational Intelligence and Security, CIS 2017*, 2018, vol. 2018-Janua, pp. 111–114, doi: 10.1109/CIS.2017.00032.

[3] M. I. Khakimyanov and F. F. Khusainov, "The information processing of dynamometer cards at controllers of automation power drives Sucker Rod Pumps," in *2016 9th International Conference on Power Drives Systems, ICPDS 2016 - Conference Proceedings*, 2016, pp. 1–6, doi: 10.1109/ICPDS.2016.7756690.

[4] X. Lv and H. Wang, "A self-evolution fault diagnosis method of sucker rod pump based on simulating dynamometer card," in *Proceedings - 2020 12th International Conference on Measuring Technology and Mechatronics Automation, ICMTMA 2020*, 2020, pp. 1–6, doi: 10.1109/ICMTMA50254.2020.00009.

[5] J. Liu, J. Feng, and X. Gao, "Fault Diagnosis of Rod Pumping Wells Based on Support Vector Machine Optimized by Improved Chicken Swarm Optimization," in *IEEE Access*, vol. 7, pp. 171598–171608, 2019, doi: 10.1109/ACCESS.2019.2956221.

[6] B. W. Hansen, "Smart Technologies for Oil Production with Rod Pumping," 2018.

[7] A. Krasovsky, "Simulation and analysis of improved direct torque control of switched reluctance machine," *Indones. J. Electr. Eng. Comput. Sci.*, vol. 18, no. 1, pp. 251-260, 2019, doi: 10.11591/ijeecs.v18.i1.pp251-260.

[8] M. S. K. Bin Jamalus, N. Md. Yusoff, and A. Hadi Sulaiman, "Simulation of dual stage thulium-doped fiber

amplifier using pump power distribution technique," *Indones. J. Electr. Eng. Comput. Sci.*, vol. 15, no. 3, p. 1203, 2019, doi: 10.11591/ijeecs.v15.i3.pp1203-1211.
[9] L. W. White, "Predicting Behavior of Sucker-Rod Pumping Systems With Optimal Control," *J. Dyn. Syst. Meas. Control*, no. October, pp. 1-17, 2017, doi: 10.1115/1.4038112.
[10] A. V. Semenov, S. I. Tecle, and A. Ziuzev, "Modeling Induction Motor Driven Sucker Rod Pump in MATLAB Simscape," in *Proceedings - 2020 Russian Workshop on Power Engineering and Automation of Metallurgy Industry: Research and Practice, PEAMI 2020*, 2020, pp. 67–71, doi: 10.1109/PEAMI49900.2020.9234336.
[11] S. I. Tecle and A. Ziuzev, "A Review on Sucker Rod Pump Monitoring and Diagnostic System," in *Proceedings - 2019 IEEE Russian Workshop on Power Engineering and Automation of Metallurgy Industry: Research and Practice, PEAMI 2019*, 2019, pp. 85–88, doi: 10.1109/PEAMI.2019.8915296.
[12] A. Wang *et al.*, "Tracking the multi-well surface dynamometer card state for a sucker-rod pump by using a particle filter," in *IET Communications*, vol. 12, no. 16, pp. 2058-2066, 2018, doi: 10.1049/iet-com.2018.5331.
[13] A. N. Ladygin, D. D. Bogachenko, V. V. Kholin, and N. A. Ladygin, "Method of Efficient Control of the Sucker-Rod Pump Electric Drive," in *2020 27th International Workshop on Electric Drives: MPEI Department of Electric Drives 90th Anniversary, IWED 2020 - Proceedings*, 2020, pp. 4-7, doi: 10.1109/IWED48848.2020.9069584.
[14] B. Zheng, X. Gao, and R. Pan, "Sucker Rod Pump Working State Diagnosis Using Motor Data and Hidden Conditional Random Fields," in *IEEE Transactions on Industrial Electronics*, vol. 67, no. 9, pp. 7919–7928, 2020, doi: 10.1109/TIE.2019.2944081.
[15] X. Li, X. Gao, C. Yuan, Y. Hou, and X. Chen, "Practical Parameter Estimator for Dynamometer Card of Rod Pumping Systems by Measuring Terminal Data of Drive Motor," in *Proceedings of the 31st Chinese Control and Decision Conference, CCDC 2019*, 2019, pp. 4074-4077, doi: 10.1109/CCDC.2019.8833370.
[16] H. Hu *et al.*, "The Development and Application of Dynamometer Card Measurement and Analysis System Based on Andriod Platform," in *Proceedings - 2016 8th International Conference on Computational Intelligence and Communication Networks, CICN 2016*, 2017, pp. 150-154, doi: 10.1109/CICN.2016.35.
[17] D. Diagnostic, "Sucker Rod Pumping Short Course," vol. 2. pp. 1–6, 2014, [Online]. Available: https://0aa73c5e-5e00-4b64-90ea-7763a66d9c30.filesusr.com/ugd/f8ee70_d4ba77a8b77e40d898037b28bebad23e.pdf.
[18] T. Sun, J. Shi, M. Dai, L. Xu, Y. Wang, and F. L. Jin, "Application of automatic gauging technology of rod pump dynamometer card in the oilfield," in *Proceedings - 2011 IEEE International Conference on Computer Science and Automation Engineering, CSAE 2011*, vol. 1, no. 1, 2011, pp. 399-403, doi: 10.1109/CSAE.2011.5953248.
[19] A. M. Zyuzev, M. V. Bubnov, and M. V. Mudrov, "Sucker-rod pump unit electric drive simulator," in *2016 2nd International Conference on Industrial Engineering, Applications and Manufacturing, ICIEAM 2016 - Proceedings*, 2016, pp. 0–3, doi: 10.1109/ICIEAM.2016.7911522.
[20] M. P. Lamoureux, "The mathematics of PDEs and the wave equation," *Seism. Imaging Summer Sch. August 7–11, 2006, Calgary*, pp. 1-39, 2006, [Online]. Available: http://www.mathtube.org/sites/default/files/lecture-notes/Lamoureux_Michael.pdf.
[21] S. C. Chapra and R. P. Canale, *Numerical Methods for Engineers*, Seventh Ed. New York: McGraw-Hill Science/Engineering/Math, 2015.
[22] T. A. Everitt, C. Oil, J. W. Jennings, and A. Texas, "An Improved Finite-Difference Calculation of Downhole Dynamometer Cards for Sucker-Rod Pumps," *SPE Prod. Eng.*, no. February, pp. 121–127, 1992, doi: 10.2118/18189-PA.
[23] E. P. Specification, "European Patent Specification," 2018.
[24] D. Houcque, *Introduction To Matlab for Engineering Students*, no. August. 2005.
[25] MatLab, *Programming Fundamentals R 2014 b*. 2014.

BIOGRAPHIES OF AUTHORS

Erwani Merry Sartika, a lecturer in the electrical engineering study program at Universitas Kristen Maranatha. She explored the field of control systems and system identification. Her work focuses on the role of automation, modeling, and simulation.

Arief Darmawan, a graduate of the Electrical Engineering Department at Universitas Kristen Maranatha in Bandung, and his area of expertise is computer programming. He was born in 1996 in Bogor and had an internship at PT Danfoss Indonesia.